Environmental Science and Pollution Research (2019) 26:1445–1454
https://doi.org/10.1007/s11356-018-3710-7

RESEARCH ARTICLE

Effective degradation of Orange G and Rhodamine B by alkali-activated hydrogen peroxide: roles of HO_2^- and $O_2^{\cdot-}$

Daiyao Wang[1] · Jing Zou[1] · Huahua Cai[1] · Yixin Huang[1] · Fei Li[1] · Qingfeng Cheng[2]

Received: 8 August 2018 / Accepted: 6 November 2018 / Published online: 13 November 2018

Abstract

Advanced oxidation processes offer effective solutions in treating wastewater from various industries. The process of alkali-activated hydrogen peroxide (H_2O_2) was superior for the treatment of alkaline dye wastewater because no additional reagents were required except H_2O_2. However, an important and interesting phenomenon had been observed that the primary reactive species were found different for degrading organic pollutants with the process of alkali-activated H_2O_2. Azo dye of Orange G (OG) and triphenylmethane dye of Rhodamine B (RhB) were chosen as the target organic pollutants. The influences of various parameters on OG and RhB degradation by alkali-activated H_2O_2 were evaluated. Furthermore, different scavengers, including ascorbic acid, methanol, *t*-butanol, isopropyl alcohol, furfuryl alcohol, and nitro blue tetrazolium, have been tested to identify the active species involved in dye degradation, and it was found that $O_2^{\cdot-}$ was mainly responsible for degrading OG, while HO_2^- anion was the primary oxidant for degrading RhB.

Keywords Hydrogen peroxide · Orange G · Rhodamine B · Hydroperoxy anion · Superoxide radical · Alkali-activated

Introduction

The effluent that was discharged from the dyeing industry was an important source of environmental pollution (Salinas et al. 2018; Wang et al. 2018). Due to the existences of dyes, the effluent was usually strongly colored. Discharging dye wastewater into receiving water bodies without effective treatment would affect the balance of the aquatic ecosystem, and even cause damage to human health because of the mutagenic, carcinogenic, and toxic effects of the dyes (Jain and Gogate 2018; Long et al. 2017). In particular, azo dyes and triphenylmethane dyes attracted special attention due to the extensive use in textile, printing, food, and cosmetic industries. Moreover, both types of dyes were characterized by the complex and steady molecular structures making them quite resistant to biological degradation and exert long-term adverse effects on the aquatic environment (Babendure et al. 2003; Sun et al. 2012; Yang et al. 2012).

With the increasing concentrations of dyes occurring in effluents, the development of degrading dyes from textile dyeing wastewater had been more and more crucial than ever. Among versatile biological, physical, and chemical technologies in pollutant treatments (Falås et al. 2016; Ganzenko et al. 2014; Li et al. 2017; Mouele et al. 2015; Rozas et al. 2016; Teh et al. 2016), advanced oxidation processes (AOPs) were one of the most attractive technologies due to the rate in pollutant removing (Benzaquén et al. 2015; Li et al. 2011; Pignatello et al. 2006; Wang et al. 2011). Several AOPs, such as TiO_2-mediated photocatalysis (Li et al. 2011), Fenton (Pignatello et al. 2006) or photo-Fenton reaction (Benzaquén et al. 2015), and Co^{2+}/ozone process (Wang et al. 2011), had been examined for the degradation of dyes. AOPs based on the activation of hydrogen peroxide (H_2O_2) produce highly powerful hydroxyl radical (·OH) and non-selectively degrade large amounts of organic pollutants. The process was

Responsible editor: Ester Heath

Electronic supplementary material The online version of this article (https://doi.org/10.1007/s11356-018-3710-7) contains supplementary material, which is available to authorized users.

✉ Jing Zou
zoujing@hqu.edu.cn; zoujing05@126.com

[1] Institute of Municipal and Environmental Engineering, College of Civil Engineering, Huaqiao University, Xiamen 361021, Fujian, People's Republic of China

[2] College of Resources and Environment, Chengdu University of Information Technology, Chengdu 610225, Sichuan, People's Republic of China

considered to be one of the most economical, simple, and effective methods (And and Gallard 1999; Asghar et al. 2015; Benitez et al. 2001; Bokare and Choi 2014, Detomaso et al. 2003, Gemeay et al. 2010, Li et al. 2013, Long et al. 2012, Nidheesh et al. 2013, Rivas et al. 2015, Sun et al. 2009). The activation of H_2O_2 with transition metal ions (Ling et al. 2010), electrolysis (Ltaïef et al. 2018), microwave irradiation (Yuan and Hong 2012), ultrasonic irradiation (Kang et al. 1999), and UV irradiation (Anipsitakis and Dionysiou 2004) had been widely used in wastewater industry to degrade the toxic organic pollutants. Nevertheless, the traditional Fenton reagent (Fe^{2+}/H_2O_2) requires strict acidic conditions (pH < 4) while many wastewaters were characterized by neutral or slightly alkaline (Bokare and Choi 2014). As for the other activation methods such as electrolysis, microwave irradiation, ultrasonic irradiation, and UV irradiation, they all required extra power which would add additional cost in practice. Therefore, a simple, efficient, and low-cost activation method is still needed for degrading organic pollutants.

Recent studies showed that H_2O_2 under alkaline conditions would be ionized to form hydroperoxy anion (HO_2^-) and decomposed to generate reactive oxygen species such as hydroxyl radical (·OH), superoxide radical ($O_2^{\cdot-}$), and singlet oxygen ($^1O_2$), which were highly efficient for the degradation of organic pollutants (Fragoso et al. 2009; Gould 1985; Hayase et al. 1984; Katafias et al. 2010; Thasilu and Karthikeyan 2016; Wright and Abbot 1993; Xu et al. 2011a; Yuan and Hong 2012). Moreover, the process of alkali-activated H_2O_2 was easily implementable since the extra reagents required in this system were only H_2O_2 and sodium hydroxide. Meanwhile, it was well known that many dye wastewaters were commonly characterized by high alkalinity (pH > 12.0) (Li et al. 2018; Prisciandaro et al. 2005; Rao et al. 2007). Thus, the process of alkali-activated H_2O_2 was highly feasible and superior for the treatment of alkaline dye wastewaters.

However, an important and interesting phenomenon had been observed that the primary reactive species were found different for degrading organic pollutants with the process of alkali-activated H_2O_2. In the research reported by Yuan et al., ·OH was regarded as the oxidizing species in microwave irradiation/H_2O_2 system under alkaline circumstance for the degradation of Rhodamine B (Yuan and Hong 2012). However, Katafias et al. found HO_2^- was the dominant oxidizing species in the reaction for the degradation of methylene blue (Katafias et al. 2010). And in the study reported by Hayase et al., HO_2^- was also suggested as the primary oxidant for the degradation of melanoidins in alkaline circumstance (Hayase et al. 1984). Moreover, Gould and co-workers found that both ·OH and $O_2^{\cdot-}$ were the primary oxidizing species in the delignification process of agricultural residues (Gould 1985). Therefore, identifying the primary oxidant responsible for organic pollutant degradation in the process of alkali-activated H_2O_2 was highly necessary. In the present study, a typical azo dye of Orange G (OG) and a common triphenylmethane dye of Rhodamine B (RhB) were chosen as the target organic pollutants, and the aims of this study were (i) to investigate the degradation efficiencies of OG and RhB by alkali-activated H_2O_2, (ii) to study the influences of operational parameters on OG and RhB degradation by alkali-activated H_2O_2, and (iii) to identify the primary oxidant responsible for OG and RhB degradation by alkali-activated H_2O_2 using quenching experiments.

Materials and methods

Materials

Chemicals including RhB, *t*-butanol, and furfuryl alcohol were purchased from Shanghai Aladdin Bio-Chem Technology Co., Ltd. OG, hydrogen peroxide (H_2O_2), sodium hydroxide (NaOH), ascorbic acid, methanol, isopropanol, and nitro blue tetrazolium (NBT) were obtained from Sinopharm Chemical Reagent Co., Ltd. All of chemicals used were analytical grade without any further purification. Stock solutions were prepared with ultrapure water (18.2 MΩ cm) produced from an ultrapure water system (Milli-Q Biocel, USA).

Experimental procedures

All batch experiments were performed in 150-mL conical beakers under light and at 25 °C. The concentrations of both OG and RhB stock solutions were 10 mM. A 10-mM OG stock solution was obtained by dissolving 0.452 g OG in 100 mL of ultrapure water. A 10-mM RhB stock solution was obtained by dissolving 0.479 g RhB in 100 mL of ultrapure water. The concentration of H_2O_2 stock solution was 900 mM. In a typical degradation experiment, a desired volume of ultrapure water and dye stock solution was initially added into the beaker, and then NaOH solution was used to adjust solution pH to the desired value. Finally, H_2O_2 stock solution was added to the above solution to initiate the reaction (H_2O_2 stock solution was prepared by the dilution of 30% H_2O_2 (9.76 M)). The total volume of the reaction solution was 100 mL. Control experiments were conducted without the addition of H_2O_2. The quenching experiments employed ascorbic acid, methanol, *t*-butanol, isopropanol, furfuryl alcohol, and NBT as quenchers, and then the desired dosages of scavengers were separately added into the beaker before dosing H_2O_2 stock solution.

At a given reaction time, 1 mL of aqueous solution was taken from the bottle by the pipette. Since H_2O_2 could not degrade OG ($pK_a = 11.5$) and RhB ($pK_a = 3.0–3.7$) under neutral pH conditions, reaction solutions in quartz cuvettes were then adjusted to neutral pH by adding 0.5 M of pH 6.0

phosphate buffer solution at a volume ratio of 1:1 to quench the degradation reactions and avoid the impact of pH on the measurements of OG and RhB.

Analysis and calculations

The absorption spectra from 200 to 800 nm of the dyes were recorded using an UV-Vis spectrophotometer (TU-1901, Persee Instruments, China). The absorption values of dyes were measured at the maximum absorbance wavelength (λ_{max}) where OG was 478 nm and RhB was 555 nm. The dye degradation efficiency and the corresponding apparent rate constant (k_{obs}) in a sample were calculated according to Eqs. (1) and (2), respectively:

$$\mathrm{DE}(\%) = \frac{C_0 - C_t}{C_0} \times 100 \quad (1)$$

$$\mathrm{Ln}(C_0/C_t) = k_{obs} \times t \quad (2)$$

where:

DE the dye degradation efficiency (%)
C_0 the initial dye concentration (mM)
C_t the residual dye concentration at reaction time of t (min) (mM)
k_{obs} the corresponding apparent rate constant (min^{-1})

Results and discussion

General observations

The effects of H_2O_2 on the degradation of OG and RhB were investigated at alkaline pH, and the results are shown in Fig. 1. Control experiments were conducted in the absence of H_2O_2, and the outcomes showed little degradation of OG and RhB. However, the degradation efficiencies of OG and RhB were tremendously accelerated by the addition of H_2O_2. About 74% of OG and 99% of RhB were respectively decomposed within 60 min at pH 11.5 and pH 13.0. Additionally, it was found that solution pH was nearly unchanged during the reaction (results not shown), which was due to the strong buffering capacity of the highly alkaline solution. Consequently, the process of alkali-activated H_2O_2 was highly effective for degrading OG and RhB. Additionally, the changes of TOC concentrations were also measured during the degradation of OG and RhB with alkaline-activated H_2O_2, and the TOC removals for OG and RhB after 60 min were respectively 10.4% and 8.3% as shown in Fig. S1.

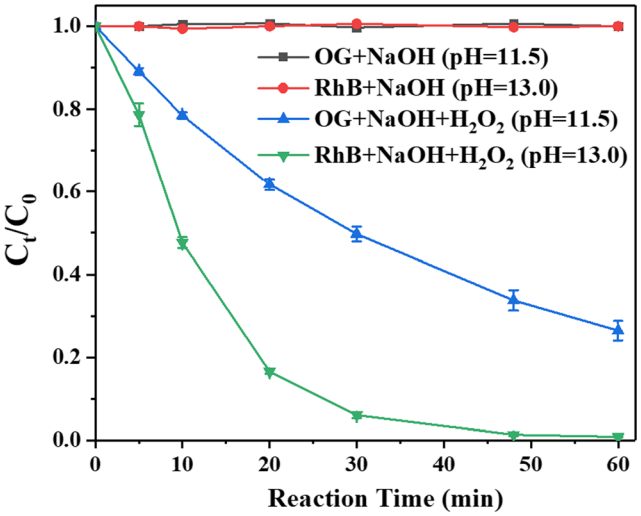

Fig. 1 Degradation of OG and RhB by alkali-activated H_2O_2. Experimental conditions: $[OG]_{initial} = 0.2$ mM or $[RhB]_{initial} = 0.2$ mM, pH = 11.5 or 13.0, $[H_2O_2]_{initial} = 36$ mM, temperature (T) = 25 ± 2 °C

Effect of solution pH

Solution pH is an important factor in AOPs based on the activation of H_2O_2, since it can significantly affect the degradation of dye pollutants (Chahbane et al. 2007; Huang et al. 2003). Figure 2 showed the influence of initial solution pH on the degradation of OG and RhB in the process of alkali-activated H_2O_2.

As shown in Fig. 2a, with the addition of 36 mM H_2O_2, the degradation efficiency of OG within 60 min was significantly increased from about 7% to 74% when solution pH was ranged from 10.0 to 11.5, and then promptly decreased to about 4% with further increasing pH to 13.0. Moreover, the kinetic of OG degradation in the pH range of 10.0–13.0 was well consistent with a second-order reaction (Fig. S2 and Tab. S2). k_{obs} of OG degradation was increased from 0.00139 to 0.02225 min^{-1} and then decreased to 0.00037 min^{-1} when solution pH ranged from 10.0 to 13.0 (Fig. 3, Fig. S2 and Tab. S2). Consequently, the optimum pH for OG degradation in the process of alkali-activated H_2O_2 was 11.5.

Figure 2b showed the effect of solution pH on RhB degradation by alkali-activated H_2O_2. When solution pH was increased from 10.0 to 13.0, the degradation efficiency of RhB within 60 min was continuously increased from about 5 to 99%. Similarly, the kinetic of RhB degradation in the pH range of 10.0–13.0 was also accorded with a second-order reaction (Fig. S2 and Tab. S2). k_{obs} of RhB degradation was continuously increased from 0.00076 to 0.09703 min^{-1} when the solution pH was ranged from 10.0 to 13.0 (Fig. 3, Fig. S2 and Tab. S2). In other words, the degradation of RhB was continuously accelerated by increasing solution pH in the pH range of 10.0–13.0. It indicated that the effect of solution pH was obviously different for the degradation of OG and RhB in the process of alkali-activated H_2O_2.

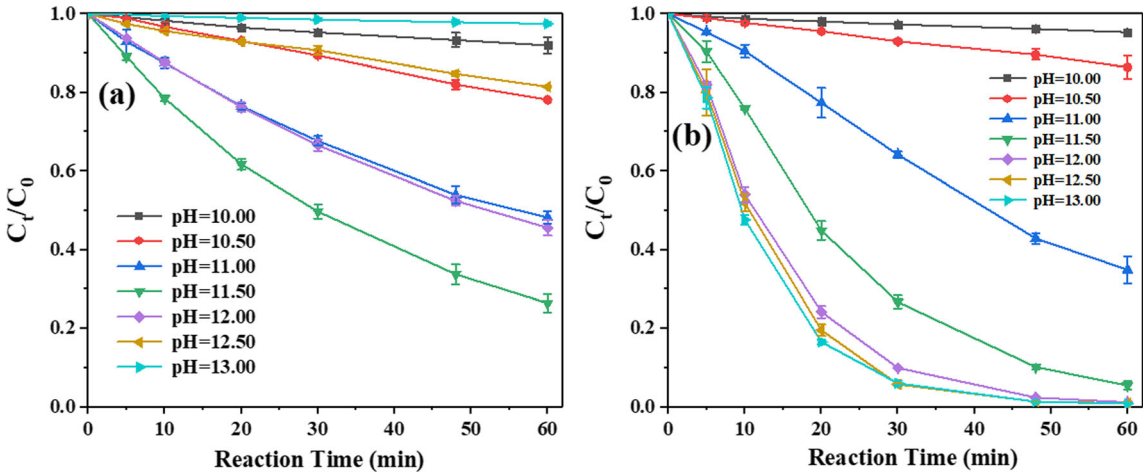

Fig. 2 Effect of initial solution pH on the degradation of **a** OG and **b** RhB by alkaline-activated H_2O_2. Experimental conditions: $[OG]_{initial} = 0.2$ mM or $[RhB]_{initial} = 0.2$ mM, $[H_2O_2]_{initial} = 36$ mM, temperature (T) = 25 ± 2 °C

Importantly, two interesting phenomena were observed in Fig. 3. One was that the optimum solution pH for OG degradation (pH = 11.5) was corresponding with the pK_a of H_2O_2 (pK_a = 11.62) (Christensen et al. 1982), and the other was that there was a positive correlation between k_{obs} of RhB degradation and the fraction of HO_2^- (αHO_2^-) in the pH range of 10.0–13.0. The stability of H_2O_2 under alkaline conditions had been reported to be pH dependent in previous literatures (Buxton et al. 1988; Christensen et al. 1982; Cui et al. 2017; Fu et al. 2017; Miao et al. 2015), and the self-decomposition of H_2O_2 tended to be fastest in the pH range of 11–12 (Qiang et al. 2002). Moreover, the primary pathways for the decomposition of H_2O_2 to generate reactive oxygen species (i.e., ·OH, $O_2^{\cdot-}$, and $^1O_2$) under alkaline conditions are shown in Eqs. (3)–(14) (Buxton et al. 1988; Christensen et al. 1982; Cui et al. 2017; Fu et al. 2017; Miao et al. 2015; Qiang et al. 2002). Additionally, HO_2^-, the product of deprotonation of H_2O_2 (Eq. (3)), had been reported to be more efficient for phenothiazine degradation (Katafias et al. 2010). As a result, the assumption that the primary oxidants for OG degradation and RhB degradation were respectively reactive oxygen species and HO_2^- was proposed in this study.

$$H_2O_2 \leftrightarrow HO_2^- + H^+ \quad pK_a = 11.62 \tag{3}$$

$$HO_2^- + H_2O_2 \rightarrow HO_2^{\cdot} + {\cdot}OH + OH^- \quad k = 3M^{-1}s^{-1} \tag{4}$$

$$HO_2^{\cdot} + {\cdot}OH \rightarrow H_2O + O_2 \quad k = 7.5 \times 10^9 M^{-1}s^{-1} \tag{5}$$

$$HO_2^{\cdot} + O_2^{\cdot-} \rightarrow H_2O_2 + O_2 \quad k = 9.7 \times 10^7 M^{-1}s^{-1} \tag{6}$$

$${\cdot}OH + O_2^{\cdot-} \rightarrow OH^- + O_2 \quad k = 1.01 \times 10^{10} M^{-1}s^{-1} \tag{7}$$

$$HO_2^{\cdot} + H_2O_2 \rightarrow H_2O + {\cdot}OH + O_2 \quad k = 0.5 \pm 0.09 M^{-1}s^{-1} \tag{8}$$

$$HO_2^{\cdot} \leftrightarrow O_2^{\cdot-} + H^+ \quad pK_a = 4.8 \tag{9}$$

$${\cdot}OH + H_2O_2 \rightarrow H_2O + O_2^{\cdot-} \quad k = 2.7 \times 10^7 M^{-1}s^{-1} \tag{10}$$

$${\cdot}OH + HO_2^- \rightarrow H_2O + O_2^{\cdot-} \quad k = 7.5 \times 10^9 M^{-1}s^{-1} \tag{11}$$

$${\cdot}OH + {\cdot}OH \rightarrow H_2O_2 \quad k = 5.5 \times 10^9 M^{-1}s^{-1} \tag{12}$$

$${\cdot}OH + O_2^{\cdot-} \rightarrow OH^- + {}^1O_2 \quad k = 8 \times 10^9 M^{-1}s^{-1} \tag{13}$$

$$HO_2^{\cdot} + HO_2^{\cdot} \rightarrow H_2O_2 + {}^1O_2 \quad k = 8.3 \times 10^5 M^{-1}s^{-1} \tag{14}$$

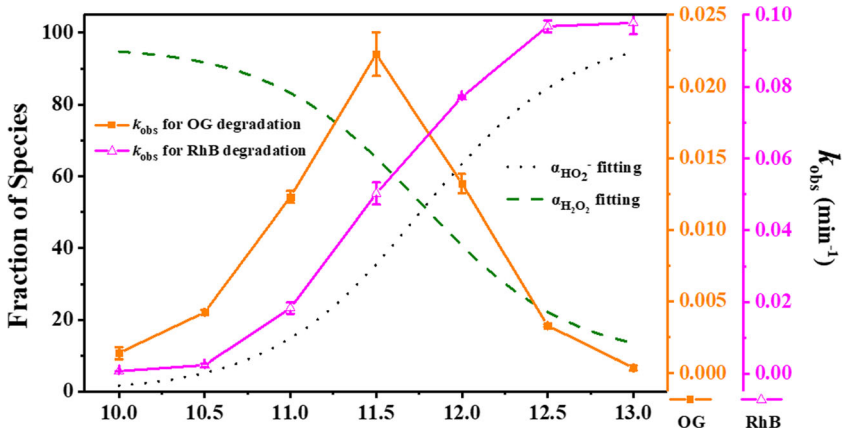

Fig. 3 Effect of solution pH on αHO_2^- and k_{obs}. Experimental conditions: $[OG]_{initial} = 0.2$ mM or $[RhB]_{initial} = 0.2$ mM, $[H_2O_2]_{initial} = 36$ mM, temperature (T) = 25 ± 2 °C

Effect of H_2O_2 concentration

Since H_2O_2 was the source of reactive oxygen species generation and HO_2^- formation (Buxton et al. 1988, Christensen et al. 1982, Cui et al. 2017, Fu et al. 2017, Miao et al. 2015, Qiang et al. 2002), the effect of H_2O_2 concentration on the degradation of OG and RhB was studied. As shown in Fig. S3(a), the degradation efficiency of OG was increased rapidly from about 24 to 91% when H_2O_2 concentration increased from 9 to 72 mM. Correspondingly, k_{obs} of OG degradation was almost linearly increased from 0.00484 to 0.04331 min^{-1} when H_2O_2 concentration increased from 9 to 72 mM (Fig. 4, Fig. S2 and Tab. S2). As shown in Fig. S3(b), the RhB degradation efficiency was augmented from 73% to near 100% when H_2O_2 concentration was increased from 9 to 72 mM. The corresponding k_{obs} was increased from 0.02077 to 0.18078 min^{-1} with the increasing H_2O_2 concentration (Fig. 4, Fig. S2 and Tab. S2). Hence, it could be inferred that more reactive oxygen species and HO_2^- were generated with higher H_2O_2 concentration, resulting in higher degradation efficiencies of OG and RhB by alkali-activated H_2O_2.

Effect of reaction temperature

Figure S4 showed the effect of reaction temperature on the degradation of OG and RhB degradation by alkali-activated H_2O_2. The degradation efficiencies of OG and RhB within 60 min were respectively about 38% and 87% when reaction temperature was 10 °C. Higher degradation efficiencies were observed when reaction temperature increased to 40 °C. The major reason was that higher temperature could enhance reactive oxygen species generation and HO_2^- formation, further enhancing the degradation of OG and RhB. In addition, the degradation of OG and RhB between 10 and 40 °C followed the second-order kinetics well (Fig. S2 and Tab. S2). k_{obs} of OG degradation and RhB degradation by alkali-activated H_2O_2 could be also calculated with Arrhenius' equation (Eq. (15)) (Sun et al. 2009).

$$k_{obs} = A\exp\left(\frac{-E}{RT}\right) \quad (15)$$

where:

- A the pre-exponential factor
- E the activation energy for the reaction (J mol^{-1})
- R universal gas constant (8.314 J mol^{-1} K^{-1})
- T the absolute temperature (K)

The plots of k_{obs} versus T and the Arrhenius plots of ln k_{obs} versus T^{-1} are shown in Fig. 5. There was a well linear relationship between ln k_{obs} and T^{-1} ($R^2 > 0.999$). The apparent activation energy of the degradation of OG and RhB by alkali-activated H_2O_2 was then calculated to be 44.48 kJ mol^{-1} and 47.37 kJ mol^{-1}, respectively. It was important to notice that the apparent activation energy of the thermal degradation of organic pollutants was usually more than 60 kJ mol^{-1} (Chen and Zhu 2007). This implied that the degradation of two dyes in aqueous solution by alkali-activated H_2O_2 was quite easy to achieve.

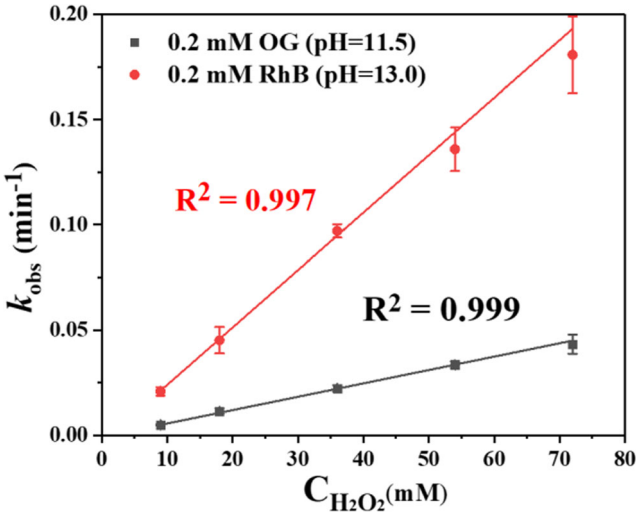

Fig. 4 Effect of H_2O_2 concentration on the degradation of OG and RhB by alkali-activated H_2O_2. Experimental conditions: $[OG]_{initial} = 0.2$ mM or $[RhB]_{initial} = 0.2$ mM, pH = 11.5 or 13.0, temperature (T) = 25 ± 2 °C

Identification of the primary reactive species

Several research groups have reported the decomposition of H_2O_2 under alkaline conditions for in situ generation of a variety of reactive oxygen species, including ·OH (Bokare and Choi 2014), $O_2^{\cdot-}$ (Li et al. 2018), and $^1O_2$ (Zhou et al. 2015), which were reactive for pollutant degradation (Eqs. (3)–(14)). To identify whether the abovementioned reactive oxygen species were the primary oxidants for the degradation of OG and RhB in alkali-activated H_2O_2, ascorbic acid, a common radical scavenger, was added (Zhou et al. 2013). As shown in Fig. 6, the degradation of OG was completely inhibited with the addition of 72 mM ascorbic acid whereas the degradation of RhB was only slightly inhibited. It could be inferred that the abovementioned reactive oxygen species (i.e., ·OH, $O_2^{\cdot-}$, and/or $^1O_2$) were the primary oxidants for OG degradation, but not for RhB degradation. On the contrary, HO_2^-, the product of deprotonation of H_2O_2 (Eq. (3)), was the primary oxidant responsible for RhB degradation by alkali-activated H_2O_2.

Moreover, methanol, *t*-butanol, and isopropyl alcohol were commonly recognized powerful ·OH scavengers, having the second-order rate constants of $9.7 \times 10^8 M^{-1}s^{-1}$, $6 \times 10^8 M^{-1}s^{-1}$, and $1.9 \times 10^9 M^{-1}s^{-1}$, respectively with ·OH (Li et al. 2018; Zhou et al. 2013; Zhou et al. 2015). Figure 7 and Fig. S5 showed the inhibition of methanol, *t*-butanol, and isopropyl alcohol on the degradation of OG and RhB.

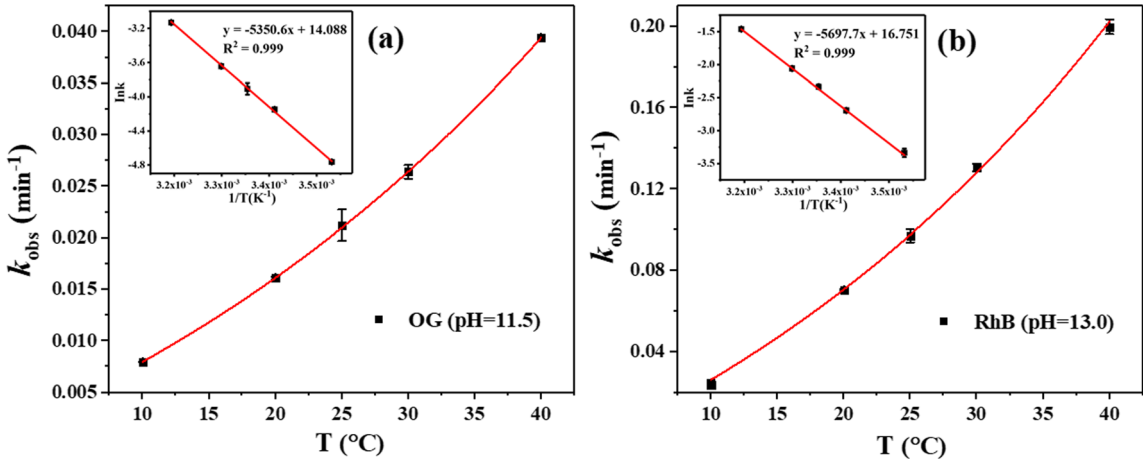

Fig. 5 Effect of reaction temperature on the degradation of **a** OG and **b** RhB by alkali-activated H_2O_2. Experimental conditions: $[OG]_{initial}$ = 0.2 mM or $[RhB]_{initial}$ = 0.2 mM, pH = 11.5 or 13.0, $[H_2O_2]_{initial}$ = 36 mM

Obviously, adding these three ·OH scavengers did not affect the degradation of OG and RhB at all, indicating that ·OH was not the primary oxidant for the degradation of OG and RhB by alkali-activated H_2O_2.

Furfuryl alcohol was generally assumed as an effective quencher for $^1O_2$ with the rate constant of $1.2 \times 10^8 M^{-1}s^{-1}$ (Zhou et al. 2015). As demonstrated in Fig. 8, adding furfuryl alcohol did not affect OG and RhB degradation at all, indicating that $^1O_2$ was also not the primary oxidant for the degradation of OG and RhB by alkali-activated H_2O_2.

NBT had been reported for detecting $O_2^{\cdot-}$ because it did not react with other active oxygen species except $O_2^{\cdot-}$ and ·OH (Peng et al. 2016; Xu et al. 2011b). As it had been demonstrated that ·OH did not play significant role in the degradation of OG and RhB (Fig. 7 and Fig. S5), NBT was used to identify $O_2^{\cdot-}$.

Figure 9a reveals the inhibitory effect on OG degradation with the addition of NBT, which was the same with the addition of ascorbic acid. These results confirmed that $O_2^{\cdot-}$ was the primary oxidant responsible for OG degradation by alkali-activated H_2O_2. Meanwhile, the characteristic UV-Vis spectrum was used to confirm the generation of $O_2^{\cdot-}$ by alkali-activated H_2O_2. The method was based on the reaction that $O_2^{\cdot-}$ could react with NBT to produce diformazan which has the characteristic absorption peak at 560 nm (Chen et al. 2010). Experimental results are displayed in Fig. 10. The purple diformazan was not found in control experiments with NBT and NaOH. However, in the test with the addition of H_2O_2, the increased absorbance between 400 and 800 nm with the reaction proceeding indicated the formation of diformazan during the degradation process. Consequently, $O_2^{\cdot-}$ was indeed generated by alkali-activated H_2O_2 and played a vital role in OG degradation. Nevertheless, Fig. 9b showed that no obvious inhibition effect on RhB degradation was observed with the addition of NBT, which was also the same with the addition of ascorbic acid. These results implied that $O_2^{\cdot-}$ was involved in RhB degradation by alkali-activated H_2O_2, but the contribution of $O_2^{\cdot-}$ to the degradation of RhB

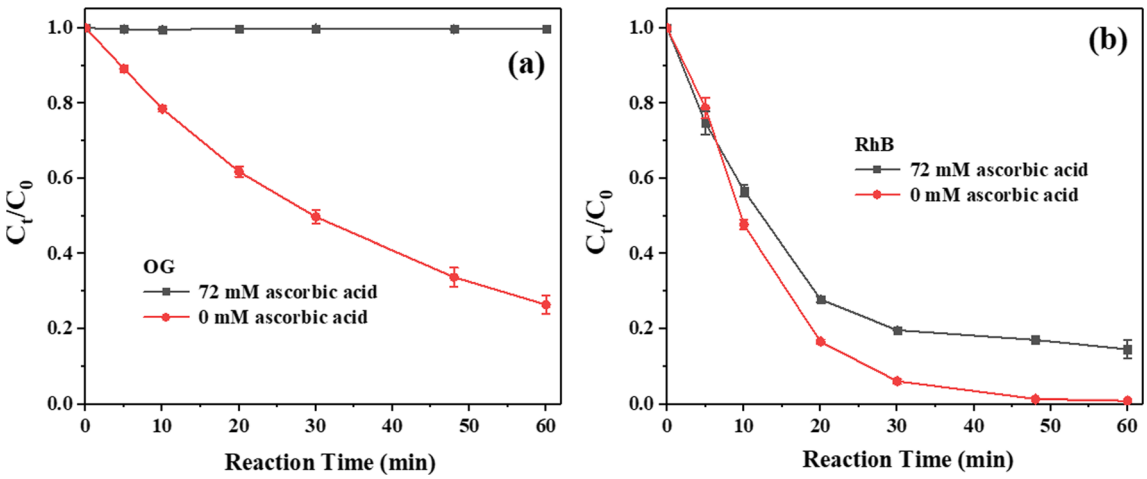

Fig. 6 Influence of ascorbic acid on the degradation of **a** OG and **b** RhB by alkali-activated H_2O_2. Experimental conditions: $[OG]_{initial}$ = 0.2 mM or $[RhB]_{initial}$ = 0.2 mM, pH = 11.5 or 13.0, $[H_2O_2]_{initial}$ = 36 mM, temperature (T) = 25 ± 2 °C

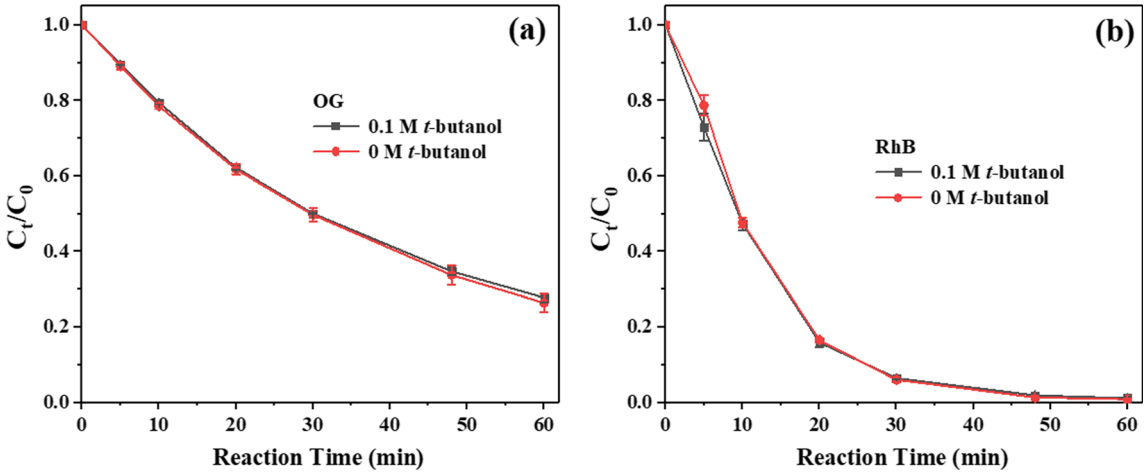

Fig. 7 Influence of *t*-butanol on the degradation of **a** OG and **b** RhB by alkali-activated H_2O_2. Experimental conditions: $[OG]_{initial} = 0.2$ mM or $[RhB]_{initial} = 0.2$ mM, pH = 11.5 or 13.0, $[H_2O_2]_{initial} = 36$ mM, temperature (T) = 25 ± 2 °C

was negligible in comparison with the contribution of HO_2^-. Moreover, although carbon tetrachloride and *p*-benzoquinone had been widely applied as $O_2^{\cdot-}$ scavengers to confirm the presence of $O_2^{\cdot-}$ (Fu et al. 2015; Li et al. 2018), it was inappropriate to use them to identify $O_2^{\cdot-}$ because of the low solubility of carbon tetrachloride and the catalytic ability of *p*-benzoquinone (Allian et al. 1994).

In summary, although all the oxidants of HO_2^-, ·OH, $O_2^{\cdot-}$, and $^1O_2$ could be generated by alkali-activated H_2O_2 via Eqs. (3)–(14) (Buxton et al. 1988; Christensen et al. 1982; Cui et al. 2017; Fu et al. 2017; Miao et al. 2015; Qiang et al. 2002), the primary oxidants responsible for the degradation of OG and RhB were different. According to the significant inhibition of ascorbic acid and NBT and the negligible inhibition of methanol, *t*-butanol, isopropyl alcohol, and furfuryl alcohol on OG degradation, the primary oxidant responsible for OG degradation was confirmed as $O_2^{\cdot-}$. On the contrary, the primary oxidant responsible for RhB degradation was confirmed as HO_2^- based on the effect of solution pH and the negligible inhibition of ascorbic acid, methanol, *t*-butanol, isopropyl alcohol, NBT, and furfuryl alcohol on RhB degradation. The difference for the primary oxidant could be mainly attributed to the chemical characteristics of OG and RhB (Tab. S1). Specifically, OG was a typical azo dye while RhB was a common triphenylmethane dye. Qi et al. (Qi et al. 2016) had reported that the degradation of AO7 was initiated by the breakdown of azo bond due to the oxidative attack of $O_2^{\cdot-}$ that generated by alkali-activated PMS. Moreover, in another study reported by Li et al., the degradation of AO7 in the process of the activation of hydrogen peroxide with carbonate was also supposed to be the breakdown of azo bond by the generated $O_2^{\cdot-}$, rather than HO_2^- (Li et al. 2018). Consequently, it could be concluded that $O_2^{\cdot-}$, rather than HO_2^-, was sensitive for the breakdown of azo bond, and was also mainly responsible for the degradation of the azo dye of OG in the process of alkali-activated H_2O_2. Earlier, Katafias et al. had reported that methylene blue, a phenothiazine dye containing four *N*-methyl groups, was decolorized by the successive nucleophilic attack

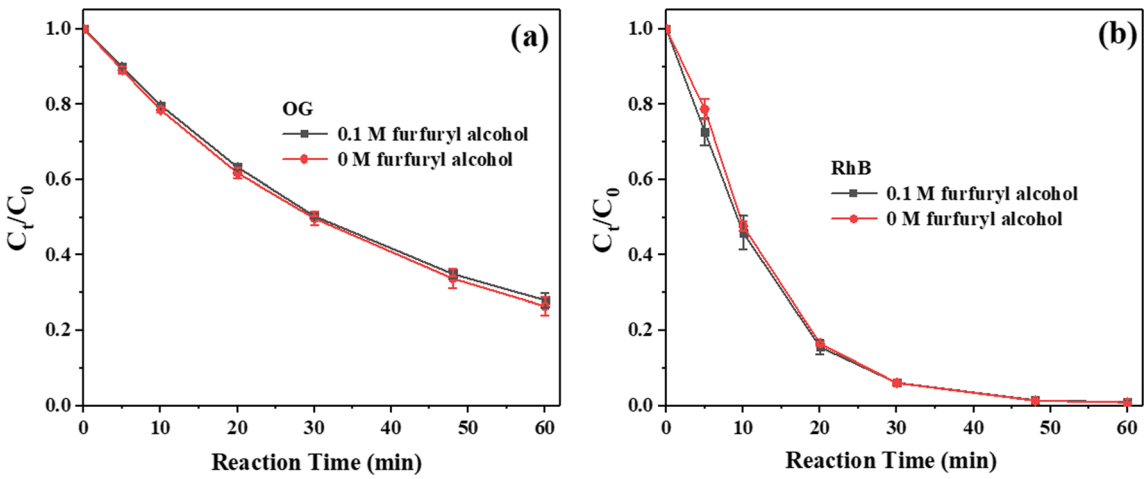

Fig. 8 Influence of furfuryl alcohol on the degradation of **a** OG and **b** RhB by alkali-activated H_2O_2. Experimental conditions: $[OG]_{initial} = 0.2$ mM or $[RhB]_{initial} = 0.2$ mM, pH = 11.5 or 13.0, $[H_2O_2]_{initial} = 36$ mM, temperature (T) = 25 ± 2 °C

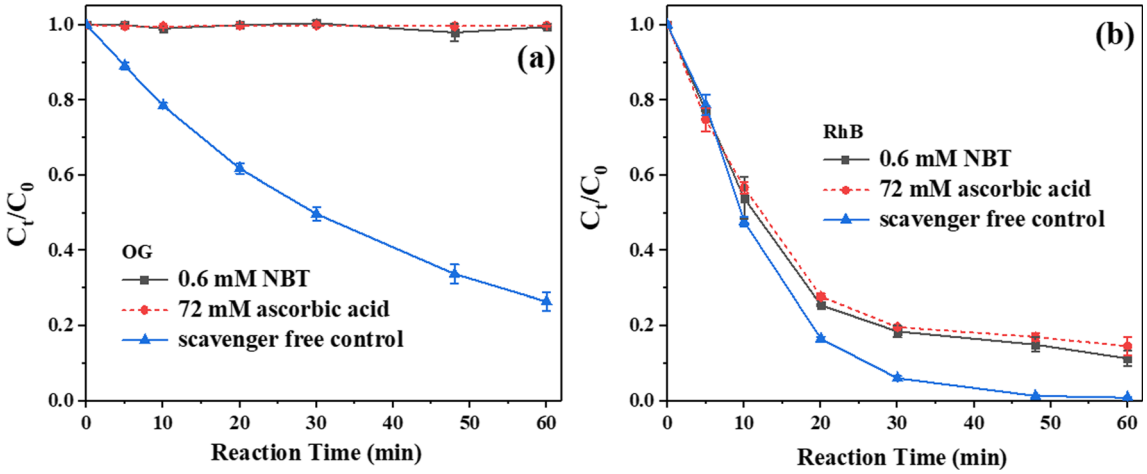

Fig. 9 Influence of NBT on the degradation of **a** OG and **b** RhB by alkali-activated H_2O_2. Experimental conditions: $[OG]_{initial}$ = 0.2 mM or $[RhB]_{initial}$ = 0.2 mM, pH = 11.5 or 13.0, $[H_2O_2]_{initial}$ = 36 mM, temperature (T) = 25 ± 2 °C

of HO_2^- on the *N*-methyl group in the process of alkali-activated H_2O_2 (Katafias et al. 2010). Since RhB was a common triphenylmethane dye containing four *N*-ethyl groups at either side of the xanthene ring, it could be inferred that the deprotonated HO_2^-, which dominated at strongly alkaline pH solutions, could be sensitive for the cleavage of *N*-ethyl group, and was also mainly responsible for the degradation of the triphenylmethane dye of RhB in the process of alkali-activated H_2O_2. Therefore, it was very meaningful to investigate the degradation of other different dyes by alkali-activated H_2O_2 in our future study.

Conclusions

In this work, the process of alkali-activated H_2O_2 was used for degrading the typical azo dye of OG and the common triphenylmethane dye of RhB in aqueous solution. The optimum solution pH for degrading of OG and RhB were pH 11.5 and pH 13.0, respectively. Moreover, the degradation of OG and RhB was significantly accelerated with the increasing of H_2O_2 concentration and reaction temperature. The major reactive oxidant for the degradation of OG by alkali-activated H_2O_2 was confirmed as $O_2^{\cdot-}$, while the HO_2^- anion was the primary oxidant for the degradation of RhB.

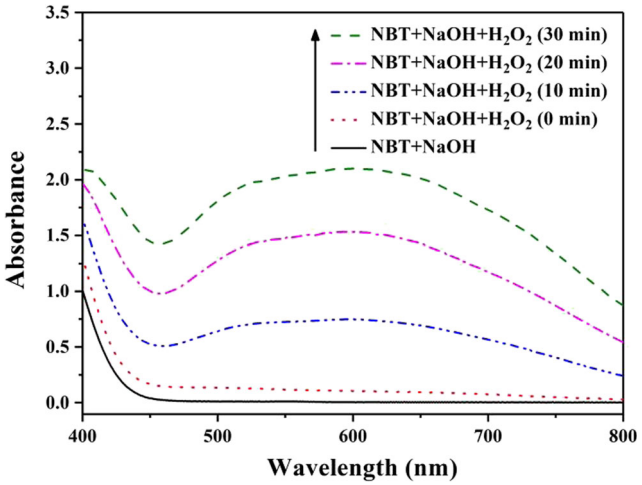

Fig. 10 UV-Vis spectra obtained from the reaction of NBT and H_2O_2 under alkaline condition. Experimental conditions: $[NBT]_{initial}$ = 0.6 mM, $[H_2O_2]_{initial}$ = 36 mM, pH = 11.5, temperature (T) = 25 ± 2 °C

Funding information This research was supported by the National Natural Science Foundation of China (No. 51708231), the China Postdoctoral Science Foundation (No. 2017M612120), the Natural Science Foundation of Fujian province (No. 14185013), and the Promotion Program for Young and Middle-aged Teacher in Science and Technology Research of Huaqiao University (No. ZQN-YX506).

References

Allian M, Germain A, Figueras F (1994) The formation of para-benzoquinone and the mechanism of the hydroxylation of phenol by hydrogen peroxide over solid acids. Catal Lett 28:409–415

And JDL, Gallard H (1999) Catalytic decomposition of hydrogen peroxide by Fe (III) in homogeneous aqueous solution: mechanism and kinetic modeling. Environ Sci Technol 33:2726–2732

Anipsitakis GP, Dionysiou DD (2004) Transition metal/UV-based advanced oxidation technologies for water decontamination. Appl Catal B 54:155–163

Asghar A, Abdul Raman AA, Wan Daud WMA (2015) Advanced oxidation processes for *in-situ* production of hydrogen peroxide/hydroxyl radical for textile wastewater treatment: a review. J Clean Prod 87:826–838

Babendure JR, Adams SR, Tsien RY (2003) Aptamers switch on fluorescence of triphenylmethane dyes. J Am Chem Soc 125:14716–14717

Benitez FJ, Beltranheredia J, Acero JL, Rubio FJ (2001) Oxidation of several chlorophenolic derivatives by UV irradiation and hydroxyl radicals. J Chem Technol Biotechnol 76:312–320

Benzaquén TB, Isla MA, Alfano OM (2015) Fenton and photo-Fenton processes for the degradation of atrazine: a kinetic study. J Chem Technol Biotechnol 90:459–467

Bokare AD, Choi W (2014) Review of iron-free Fenton-like systems for activating H_2O_2 in advanced oxidation processes. J Hazard Mater 275:121–135

Buxton GV, Greenstock CL, Helman WP, Ross AB (1988) Critical review of rate constants for reactions of hydrated electrons, hydrogen atoms and hydroxyl radicals in aqueous solution. J Phys Chem Ref Data 17:513–886

Chahbane N, Popescu D, Mitchell DA, Chanda A, Lenoir D, Ryabov AD, Schramm K, Collins TJ (2007) Fe^{III}-TAML-catalyzed green oxidative degradation of the azo dye Orange II by H_2O_2 and organic peroxides: products, toxicity, kinetics, and mechanisms. Green Chem 9:49–57

Chen J, Zhu L (2007) Heterogeneous UV-Fenton catalytic degradation of dyestuff in water with hydroxyl-Fe pillared bentonite. Catal Today 126:463–470

Chen YS, Liu BL, Chang YN (2010) Bioactivities and sensory evaluation of Pu-erh teas made from three tea leaves in an improved pile fermentation process. J Biosci Bioeng 109:557–563

Christensen H, Sehested K, Corfitzen H (1982) Reaction of hydroxyl radical with hydrogen peroxide at ambient and elevated temperatures. J Phys Chem 86:1588–1590

Cui H, Gu X, Lu S, Fu X, Zhang X, Fu GY, Qiu Z, Sui Q (2017) Degradation of ethylbenzene in aqueous solution by sodium percarbonate activated with EDDS-Fe(III) complex. Chem Eng J 309:80–88

Detomaso A, Lopez A, Lovecchio G, Mascolo G, Curci R (2003) Practical applications of the Fenton reaction to the removal of chlorinated aromatic pollutants. Environ Sci Pollut Res 10:379–384

Falås P, Wick A, Castronovo S, Habermacher J, Ternes TA, Joss A (2016) Tracing the limits of organic micropollutant removal in biological wastewater treatment. Water Res 95:240–249

Fragoso CT, Battisti R, Miranda C, de Jesus PC (2009) Kinetic of the degradation of C.I. food yellow 3 and C.I. food yellow 4 azo dyes by the oxidation with hydrogen peroxide. J Mol Catal A 301:93–97

Fu X, Gu X, Lu S, Miao Z, Xu M, Zhang X, Qiu Z, Sui Q (2015) Benzene depletion by Fe^{2+}-catalyzed sodium percarbonate in aqueous solution. Chem Eng J 267:25–33

Fu X, Gu X, Lu S, Sharma VK, Brusseau ML, Xue Y, Danish M, Fu GY, Qiu Z, Sui Q (2017) Benzene oxidation by Fe(III)-activated percarbonate: matrix-constituent effects and degradation pathways. Chem Eng J 309:22–29

Ganzenko O, Huguenot D, van Hullebusch ED, Esposito G, Oturan MA (2014) Electrochemical advanced oxidation and biological processes for wastewater treatment: a review of the combined approaches. Environ Sci Pollut Res 21:8493–8524

Gemeay AH, Mansour IA, El-Sharkawy RG, Zaki AB (2010) Kinetics of the oxidative degradation of thionine dye by hydrogen peroxide catalyzed by supported transition metal ions complexes. J Chem Technol Biotechnol 79:85–96

Gould JM (1985) Studies on the mechanism of alkaline peroxide delignification of agricultural residues. Biotechnol Bioeng 27:225–231

Hayase F, Kim SB, Kato H (1984) Decolorization and degradation products of the melanoidins by hydrogen peroxide. Agric Biol Chem 48: 2711–2717

Huang Y, Ma W, Li J, Mingming Cheng A, Zhao J, Wan L, Yu JC (2003) A novel β-CD-hemin complex photocatalyst for efficient degradation of organic pollutants at neutral pHs under visible irradiation. J Phys Chem B 107:1071–1072

Jain SN, Gogate PR (2018) Efficient removal of Acid Green 25 dye from wastewater using activated Prunus Dulcis as biosorbent: batch and column studies. J Environ Manag 210:226–238

Kang J, Hung HM, Lin AA, Hoffmann MR (1999) Sonolytic destruction of methyl *tert*-butyl ether by ultrasonic irradiation: the role of O_3, H_2O_2, frequency, and power density. Environ Sci Technol 33:3199–3205

Katafias A, Lipińska M, Strutyński K (2010) Alkaline hydrogen peroxide as a degradation agent of methylene blue-kinetic and mechanistic studies. React Kinet Mech Catal 101:251–266

Li H, Gong Y, Huang Q, Hui Z (2013) Degradation of Orange II by UV-assisted advanced Fenton process: response surface approach, degradation pathway, and biodegradability. Ind Eng Chem Res 52: 15560–15567

Li Q, Xue DX, Zhang YF, Zhang ZH, Wang Q, Gao Z, Bai J (2017) A copper-organic framework as scavenger towards organic dyes pollutants via physical adsorption and visible-light photodegradation. Inorg Chem Commun 85:78–83

Li W, Li D, Meng S, Chen W, Fu X, Shao Y (2011) Novel approach to enhance photosensitized degradation of Rhodamine B under visible light irradiation by the $Zn_xCd_{1-x}S/TiO_2$ nanocomposites. Environ Sci Technol 45:2987–2993

Li Y, Li L, Chen Z, Zhang J, Gong L, Wang Y, Zhao H, Mu Y (2018) Carbonate-activated hydrogen peroxide oxidation process for azo dye decolorization: process, kinetics, and mechanisms. Chemosphere 192:372–378

Ling SK, Wang S, Peng Y (2010) Oxidative degradation of dyes in water using Co^{2+}/H_2O_2 and Co^{2+}/peroxymonosulfate. J Hazard Mater 178:385–389

Long X, Yang Z, Wang H, Chen M, Peng K, Zeng Q, Xu A (2012) Selective degradation of Orange II with the cobalt(II)-bicarbonate-hydrogen peroxide system. Ind Eng Chem Res 51:11998–12003

Long X, Pan Q, Wang C, Wang H, Li H, Li X (2017) Microbial fuel cell-photoelectrocatalytic cell combined system for the removal of azo dye wastewater. Bioresour Technol 244:182–191

Ltaïef AH, Sabatino S, Proietto F, Ammar S, Gadri A, Galia A, Scialdone O (2018) Electrochemical treatment of aqueous solutions of organic pollutants by electro-Fenton with natural heterogeneous catalysts under pressure using Ti/IrO_2-Ta_2O_5 or BDD anodes. Chemosphere 202:111–118

Miao Z, Gu X, Lu S, Brusseau ML, Zhang X, Fu X, Danish M, Qiu Z, Sui Q (2015) Enhancement effects of chelating agents on the degradation of tetrachloroethene in Fe(III) catalyzed percarbonate system. Chem Eng J 281:286–294

Mouele ES, Tijani JO, Fatoba OO, Petrik LF (2015) Degradation of organic pollutants and microorganisms from wastewater using different dielectric barrier discharge configurations-a critical review. Environ Sci Pollut Res 22:18345–18362

Nidheesh PV, Gandhimathi R, Ramesh ST (2013) Degradation of dyes from aqueous solution by Fenton processes: a review. Environ Sci Pollut Res 20:2099–2132

Peng J, Shi H, Li J, Wang L, Wang Z, Gao S (2016) Bicarbonate enhanced removal of triclosan by copper(II) catalyzed Fenton-like reaction in aqueous solution. Chem Eng J 306:484–491

Pignatello JJ, Oliveros E, MacKay A (2006) Advanced oxidation processes for organic contaminant destruction based on the Fenton reaction and related chemistry. Crit Rev Environ Sci Technol 36:1–84

Prisciandaro M, Mazziotti DCG, Vegliò F (2005) Development of a reliable alkaline wastewater treatment process: optimization of the pretreatment step. Water Res 39:5055–5063

Qi C, Liu X, Ma J, Lin C, Li X, Zhang H (2016) Activation of peroxymonosulfate by base: implications for the degradation of organic pollutants. Chemosphere 151:280–288

Qiang Z, Chang JH, Huang CP (2002) Electrochemical generation of hydrogen peroxide from dissolved oxygen in acidic solutions. Water Res 36:85–94

Rao AG, Reddy TS, Prakash SS, Vanajakshi J, Joseph J, Sarma PN (2007) pH regulation of alkaline wastewater with carbon dioxide: a case study of treatment of brewery wastewater in UASB reactor coupled with absorber. Bioresour Technol 98:2131–2136

Rivas FJ, Kolaczkowski ST, Beltran FJ, Mclurgh DB (2015) Hydrogen peroxide promoted wet air oxidation of phenol: influence of operating conditions and homogeneous metal catalysts. J Chem Technol Biotechnol 74:390–398

Rozas O, Vidal C, Baeza C, Jardim WF, Rossner A, Mansilla HD (2016) Organic micropollutants (OMPs) in natural waters: oxidation by UV/H_2O_2 treatment and toxicity assessment. Water Res 98:109–118

Salinas T, Durruty I, Arciniegas L, Pasquevich G, Lanfranconi M, Orsi I, Alvarez V, Bonanni S (2018) Design and testing of a pilot scale magnetic separator for the treatment of textile dyeing wastewater. J Environ Manag 218:562–568

Sun M, Chen G, Zhang Y, Wei Q, Ma Z, Du B (2012) Efficient degradation of azo dyes over Sb_2S_3/TiO_2 heterojunction under visible light irradiation. Ind Eng Chem Res 51:2897–2903

Sun S, Li C, Sun J, Shi S, Fan M, Zhou Q (2009) Decolorization of an azo dye Orange G in aqueous solution by Fenton oxidation process: effect of system parameters and kinetic study. J Hazard Mater 161: 1052–1057

Teh CY, Budiman PM, Shak KPY, Wu TY (2016) Recent advancement of coagulation-flocculation and its application in wastewater treatment. Ind Eng Chem Res 55:4363–4389

Thasilu K, Karthikeyan J (2016) Chemical oxidation for degradation of textile dyes using hydrogen peroxide. Int J Circ Theor App 9:9055–9062

Wang J, Zhang T, Mei Y, Pan B (2018) Treatment of reverse-osmosis concentrate of printing and dyeing wastewater by electro-oxidation process with controlled oxidation-reduction potential (ORP). Chemosphere 201:621–626

Wang Z, Yuan R, Guo Y, Xu L, Liu J (2011) Effects of chloride ions on bleaching of azo dyes by Co^{2+}/oxone reagent: kinetic analysis. J Hazard Mater 190:1083–1087

Wright P, Abbot J (1993) The oxidation of cinnamaldehyde with alkaline hydrogen peroxide. In J Chem Kinet 25:901–911

Xu A, Li X, Xiong H, Yin G (2011a) Efficient degradation of organic pollutants in aqueous solution with bicarbonate-activated hydrogen peroxide. Chemosphere 82:1190–1195

Xu H, Xu W, Wang J (2011b) Degradation kinetics of azo dye Reactive Red SBE wastewater by complex ultraviolet and hydrogen peroxide process. Environ Prog Sustain Energy 30:208–215

Yang Z, Wang H, Chen M, Luo M, Xia D, Xu A, Zeng Q (2012) Fast degradation and biodegradability improvement of Reactive Brilliant Red X-3B by the cobalt(II)/bicarbonate/hydrogen peroxide system. Ind Eng Chem Res 51:11104–11111

Yuan NN, Hong J (2012) The research on Rhodamine B degradation in MW/H_2O_2 system under alkaline environment. Appl Mech Mater 105-107:1505–1508

Zhou L, Song W, Chen Z, Yin G (2013) Degradation of organic pollutants in wastewater by bicarbonate-activated hydrogen peroxide with a supported cobalt catalyst. Environ Sci Technol 47:3833–3839

Zhou Y, Jiang J, Gao Y, Ma J, Pang S, Li J, Lu X, Yuan L (2015) Activation of peroxymonosulfate by benzoquinone: a novel nonradical oxidation process. Environ Sci Technol 49:12941–12950